Accretion disks around black holes with account of magnetic fields *

Gennady Bisnovatyi-Kogan
Space Research Institute RAN, Moscow, Russia
and
Joint Institute of Nuclear Researches, Dubna, Russia

Abstract. Accretion disks are observed in young stars, cataclysmic variables, binary X-ray sources et al. Accretion disk theory was first developed as a theory with the local heat balance, where the whole energy produced by a viscous heating was emitted to the sides of the disk. Important part of this theory was the phenomenological treatment of the turbulent viscosity, known the " alpha" prescription, where the $(r\phi)$ component of the stress tensor was connected with the pressure as αP. Sources of turbulence in the accretion disk are discussed, including hydrodynamic turbulence, convection and magnetic field role. Optically thin solution and advective disks are considered. Related problems of mass ejection from magnetized accretion disks and jet formation are discussed.

Keywords: accretion disk, X-ray source, jet

1. Introduction

Accretion is the main source of energy in many astrophysical objects, including different types of binary stars, binary X-ray sources, most probably quasars and active galactic nuclei (AGN). Accretion onto stars, including neutron stars, terminates at an inner boundary. This may be the stellar surface, or the outer boundary of a magnetosphere for strongly magnetized stars. We may be sure in this case, that all gravitational energy of the falling matter will be transformed into heat and radiated outward.

The situation is quite different for sources containing black holes, which are discovered in some binary X-ray sources in the galaxy, as well as in many AGN. Here matter is falling to the horizon, from where no radiation arrives, so all luminosity is formed on the way to it. A high efficiency of accretion into a black hole takes place only when matter is magnetized (Schwartzman, 1971), or has a large angular momentum, when accretion disk is formed.

Intensive development of the accretion disk theory began after birth of the X-ray astronomy, when luminous X-ray sources in binary systems

* Partial funding provided by RFBR grant 02-02-16900, INTAS grant 00491, and Astronomy Programm "Nonstationary phenomena in astrophysics"

have been discovered, in which accretion was the only possible way of the energy production. The X-ray astronomy was born after the rocket launch in 1961 in USA by the group of physicists headed by R. Giacconi. The first and the brightest X-ray source outside the solar system, Sco X-1, was discovered during this flight. In subsequent time the main discoveries in X-ray astronomy have been done from satellites. The main discovery of the first X-ray satellite UHURU, launched in 1970 had been X-ray pulsars - neutron stars in binary systems. The fundamental importance has also a discovery of the first real black hole candidate in the Cyg X-1 binary source. The next X-ray satellite EINSTEIN, launched in 1978 had a good angular resolution and sensitivity, and more than 50 000 new sources, mainly extragalactic, had been discovered there. These two satellites had been also constructed in the team headed by R. Giacconi.

In subsequent years more than 20 X-ray satellites had been launched, and the most advanced ones CHANDRA (USA) and NEWTON (ESA) are operating now.

2. Standard accretion disk model

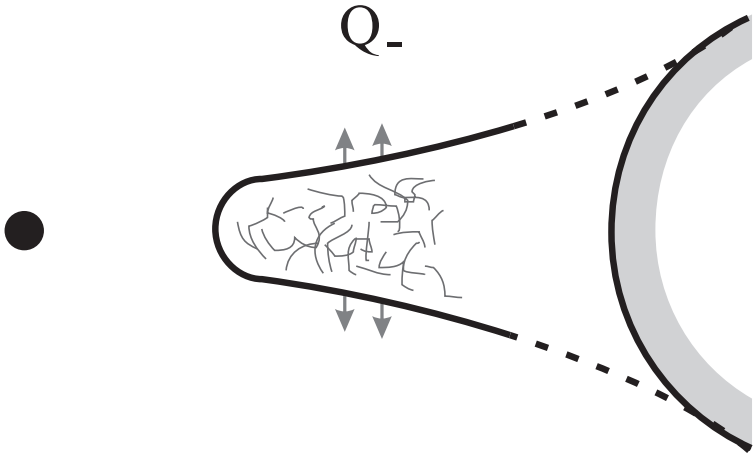

Figure 1. Schematic picture of a disc accretion into a black hole in the standard model.

The small thickness of the disk in comparison with its radius $h \ll r$ indicate to small importance of the pressure gradient ∇P in comparison with gravity and inertia forces. That leads to a simple radial equilibrium equation denoting the balance between the last two forces occuring when the angular velocity of the disk Ω is equal to the Keplerian one Ω_K,

$$\Omega = \Omega_K = \left(\frac{GM}{r^3}\right)^{1/2}. \quad (1)$$

In the "standard" accretion disk model the relation (1) is suggested to be fulfilled all over the disk, with an inner boundary at the last stable orbit, $r_{in} = 3r_g$, $r_g = 2GM/c^2$ is the gravitational Schwarzschild radius of a black hole.

The equilibrium equation in the vertical z-direction is determined by a balance between the gravitational force and pressure gradient, which for a thin disk leads to algebraic one, determining the half-thickness of the disk as

$$h \approx \frac{1}{\Omega_K}\left(2\frac{P}{\rho}\right)^{1/2}. \quad (2)$$

The ϕ component of the Navier-Stokes equation has an integral in a stationary case which represents the conservation of angular momentum

$$\dot{M}(j - j_{in}) = -2\pi r^2\, 2ht_{r\phi}, \quad t_{r\phi} = \eta r\frac{d\Omega}{dr}. \quad (3)$$

Here $j = v_\phi r = \Omega r^2$ is the specific angular momentum, $t_{r\phi}$ is the component of the viscous stress tensor, $\dot{M} > 0$ is a mass accretion rate, j_{in} is an integration constant. Multiplication of j_{in} by $\dot{M}$, gives a difference between viscous and advective flux of the angular momentum in the disk. For the accretion into a black hole it is usually assumed, that on the last stable orbit the gradient of the angular velocity is zero, corresponding to zero viscous momentum flux. In that case

$$j_{in} = \Omega_K r_{in}^2, \quad (4)$$

which is the Keplerian angular momentum of the matter on the last stable orbit.

The choice of the viscosity coefficient is the most difficult and speculative aspect of the accterion disk theory. Observations of X-ray binaries had shown, that there should be high viscosity in the accretion disks. In the paper of Shakura (1972) it was suggested, that matter in the disk is turbulent, and described by a viscous stress tensor, parametrized as

$$t_{r\phi} = -\alpha\rho v_s^2 = -\alpha P, \quad (5)$$

where α is a dimensionless constant and v_s is the sound speed. This simple parametrization corresponds to a turbulent viscosity coefficient $\eta_t \approx \rho v_t l$ with an average turbulent velocity v_t and mean free path

of the turbulent element l. It follows from the definition of $t_{r\phi}$ in (3), when we take $l \approx h$ from (2)

$$t_{r\phi} = \rho v_t h r \frac{d\Omega}{dr} \approx \rho v_t v_s = -\alpha \rho v_s^2, \tag{6}$$

where a coefficient $\alpha < 1$ relates the turbulent and sound speeds $v_t = \alpha v_s$. The presentations of $t_{r\phi}$ in (5) and (6) are equivalent. Only when the angular velocity differs considerably from the Keplerian is the first relation, on the right-hand side of (6), preferable. That does not appear (by definition) in the standard theory, but may happen when advective terms are included.

Development of a turbulence in the accretion disk cannot be justified simply, because a Keplerian disk is stable in linear approximation to the development of axially symmetric perturbations, conserving the angular momentum. It was suggested by Ya.B.Zeldovich, that in presence of very large Reynolds number $\mathrm{Re} = \frac{\rho v l}{\eta}$ the amplitude of perturbations at which nonlinear effects become important is very low, so in this situation turbulence may develop due to nonlinear instability even when the disk is stable in linear approximation. Another source of viscous stresses may arise from a magnetic field, but as was indicated by Shakura (1972), that magnetic stresses cannot exceed the turbulent ones.

It was shown by Bisnovatyi-Kogan and Blinnikov (1977), that inner regions of a highly luminous accretion discs where pressure is dominated by radiation, are unstable to vertical convection. Development of this convection produce a turbulence, needed for a high viscosity (and also leads to formation of a hot corona above this region of the disk). In the colder regions with incomplete ionization a behaviour of the accretion disk becomes more complicated, with a non-unique solutions, and convective instability (Cannizzo, Ghosh & Wheeler, 1982).

For Keplerian angular velocity the angular momentum per unit mass $j = \omega r^2 \sim r^{1/2}$ is growing outside. In this respect it is similar to the viscid flow between two rotating cylinders (Taylor experiment), when the inner cylinder is at rest. Phenomenological analysis of the Taylor experiment, and the onset of turbulence in the "stable" case of the inner cylinder at rest had been done by Zeldovich (1981).

There are arguments, both experimental and theoretical, supporting the hydrodynamic origin of the accretion disk turbulence. Non-radial perturbations ($\sim e^{im\phi}$) with a high azimuthal number $m > R/h$ are only slightly influenced by the rotation, so development of shear instability is possible for large m. The effective length in this case is $l_{eff} \sim h^2/R$, so the critical $Re_* = \rho v l_{eff}/\eta \approx 10^3$ corresponds to the actual $Re = \rho v h/\eta \approx m Re_*$. In the Taylor experiment the develop-

ment of turbulence started at $Re = 10^5$. Analytically a local shear instability in the stratified accretion disk was found by Richards et al. (2001), similar results have been obtained earlier (see Glatzel (1991) and references therein).

Magnetorotational instability of Velikhov (1959) & Chandrasekhar (1960) was advocated by Balbus & Hawley (1998). Their numerical experiments which failed to find a development of hydrodynamic shear instability could not reach the required $Re \sim 10^5$ in their simulations due to high numerical viscosity. In real astrophysical objects Re could reach 10^{10}, and become even higher. Results of recent numerical simulations (Kuznetsov et al., 2004) confirm the idea of non-linear hydrodynamic instability.

With alpha- prescription of viscosity the equation of angular momentum conservation is written in the plane of the disk as

$$\dot{M}(j - j_{in}) = 4\pi r^2 \alpha P_0 h. \tag{7}$$

When angular velocity is far from Keplerian the relation (3) is valid with a coefficient of a turbulent viscosity

$$\eta = \frac{2}{3}\alpha \rho_0 v_{s0} h, \tag{8}$$

where values with the index "0" denotes the plane of the disk.

In the standard theory a heat balance is local, what means that all heat produced by viscosity in the ring between r and $r + dr$ is radiated through the sides of disk at the same r, see Fig.1. The heat production rate Q_+ related to the surface unit of the disk is written as

$$Q_+ = h\, t_{r\phi} r \frac{d\Omega}{dr} = \frac{3}{8\pi}\dot{M}\frac{GM}{r^3}\left(1 - \frac{j_{in}}{j}\right). \tag{9}$$

Heat losses by a disk depend on its optical depth. The first standard disk model of Shakura (1972) considered a geometrically thin disk as an optically thick in a vertical direction. That implies energy losses Q_- from the disk due to a radiative conductivity, after a substitution of the differential eqiation of a heat transfer by an algebraic relation

$$Q_- \approx \frac{4}{3}\frac{acT^4}{\kappa\Sigma}. \tag{10}$$

Here a is the usual radiation energy-density constant, c is a speed of light, T is a temperature in the disk plane, κ is a matter opacity, and a surface density

$$\Sigma = 2\rho h, \tag{11}$$

here and below ρ, T, P without the index "0" are related to the disk plane. The heat balance equation is represented by a relation

$$Q_+ = Q_-, \tag{12}$$

A continuity equation in the standard model of the stationary accretion flow is used for finding of a radial velocity v_r

$$v_r = \frac{\dot{M}}{4\pi r h \rho} = \frac{\dot{M}}{2\pi r \Sigma}. \tag{13}$$

Equations (1),(2), (7),(11), (12), completed by an equation of state $P(\rho, T)$ and relation for the opacity $\kappa = \kappa(\rho, T)$ represent a full set of equations for a standard disk model. For power low equations of state of an ideal gas $P = P_g = \rho \mathcal{R} T$ ($\mathcal{R}$ is a gas constant), or radiation pressure $P = P_r = \frac{aT^4}{3}$, and opacity in the form of electron scattering κ_e, or Karammer's formula κ_k, the solution of a standard disk accretion theory is obtained analytically (Shakura, 1972; Novikov, Thorne, 1973; Shakura, Sunyaev, 1973). The structure of the accretion disk around the black hole in the standard model is represented in Fig.2.

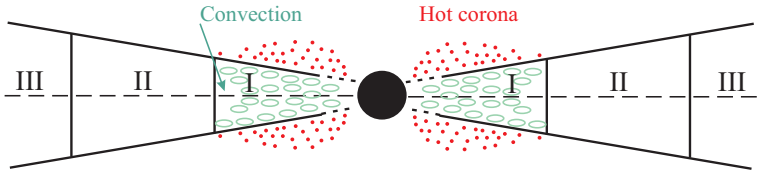

Figure 2. Sketch of picture of a disk accretion on to a black hole at sub-critical luminosity, from Bisnovatyi-Kogan (1985).

3. Observational evidences of the existence of Black Holes

3.1. Observational identification of black holes

Black holes (BH) of stellar masses have been observed in the galactic binary X-ray sources, and supermassive BH (SBH) had been found in the nuclei of active galaxies (AGN), having masses $10^7 - 10^9$ solar masses. In the galactic binary X-ray sources masses have been measured on the base of Kepler law: the compact stellar object is qualified as BH if its mass exceeds the mass of a stable neutron star, about 2.5 solar masses. X-ray binaries in our Galaxy containing black hole with low mass companion show global accretion disk instabilities, observed as soft X-ray transients - X-ray novae. The light curves of two X-ray novae in optical and X-ray bands are shown in Figs.3,4, see also review

of Cherepashchuk (2000). The mass functions of the compact object in X-ray novae, containing black holes are 3 – 6 Solar masses.

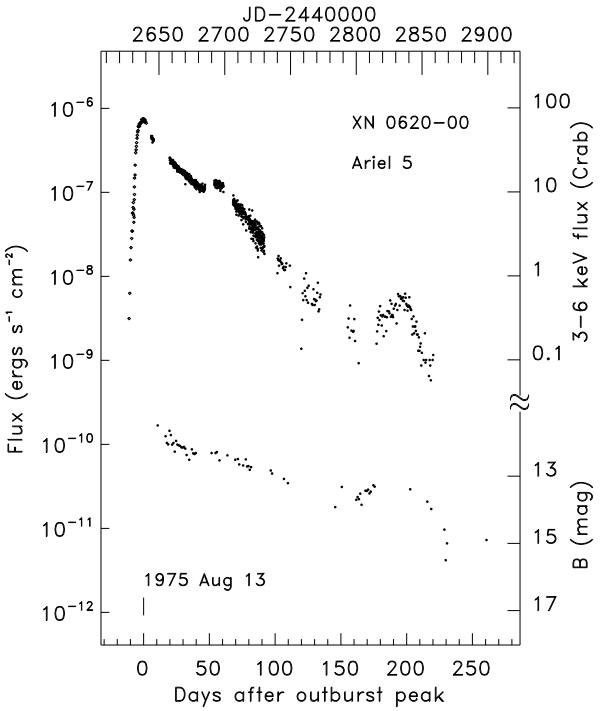

Figure 3. X-ray and optical light curves of the black-hole LMXBT A0620-00 (from Chen et al. 1997).

SBH in AGN are found by optical, X-ray and radio observations. Optical observations show strong concentration of light to the center, and existence of the accretion disk by the distribution of rotational velocity around the center. The example of such curve for the galaxy M87 with the mass of SBH about three billion solar masses is given in Fig.5 from Macchetto et al.(1997), see also Ho (1999). X-ray observations have revealed an existence of very broad emission Fe Kα lines in the X-ray spectra of AGN. The width corresponding to about one third of the speed of light may originate only near the relativistic object. The shape of the line is fitted well by the radiation from the accretion disk around SBH, which may be described by Schwarzschild or Kerr metric. This spectrum given in Fig.6 is representing the composite spectrum of Seyfert 1 galactic nuclei, obtained by Nandra et al.(1997). The most precise measurements have been done by radio VLBI observations of the water maser line from the nucleus of the Seyfert galaxy NGC 4258. The Keplerian rotational curve is obtained with very high accuracy

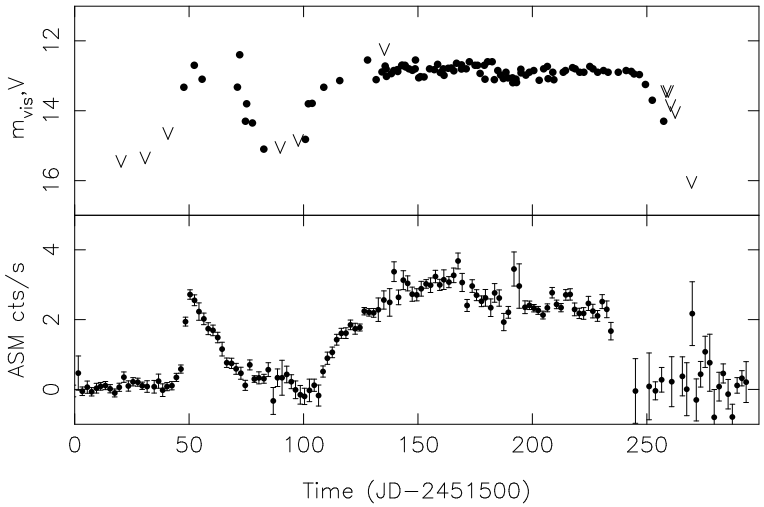

Figure 4. X-ray and optical light curves of the black-hole LMXBT XTE J1118+48 (adapted from Lasota, 2001). The 'black-hole' classification here requires confirmation.

(< 1%), implying the mass of 36 millions of solar masses within 0.13 pc. This rotational curve is represented in Fig.7 from Ho (1999).

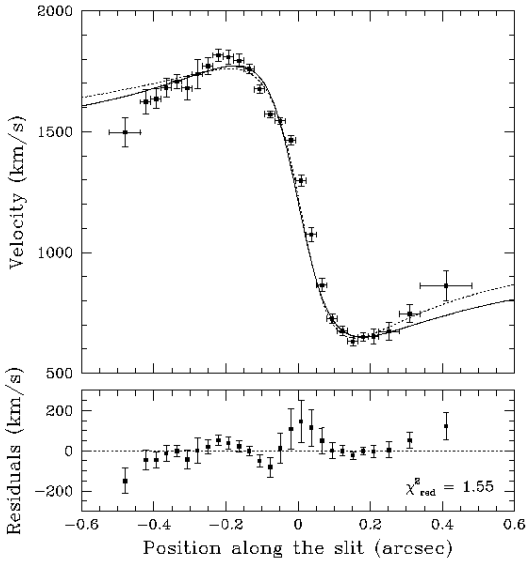

Figure 5. Optical emission-line rotation curve for the nuclear disk in M87. The two curves in the upper panel correspond to Keplerian thin disk models, and the bottom panel shows the residuals for one of the models, from Macchetto et al. (1999).

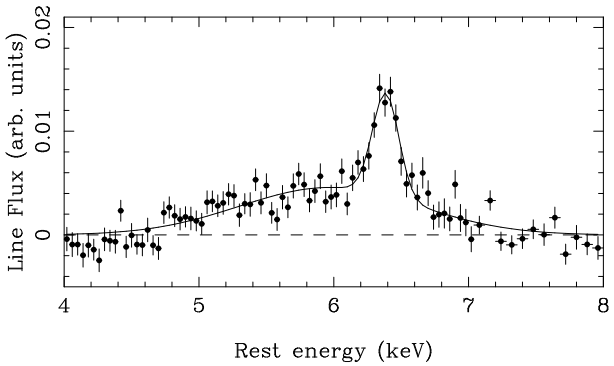

Figure 6. The Fe K line in the composite spectrum of Seyfert 1 nuclei. The solid line is a fit to the line profile using two Gaussians, a narrow component centered at 6.4 keV and a much broader, redshifted component, from Nandra et al. (1997).

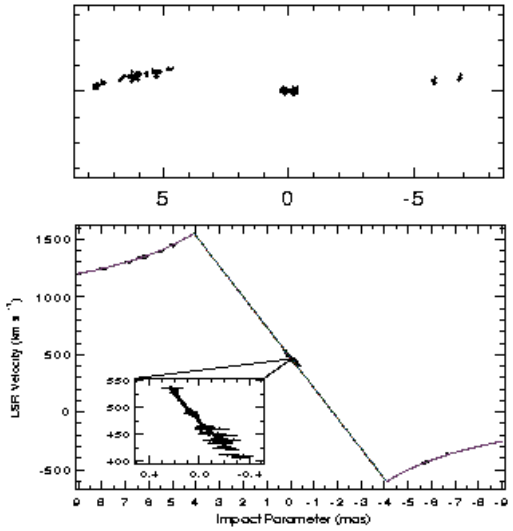

Figure 7. Water maser emission in NGC 4258 (Miyoshi et al. 1995). Top: spatial distribution of the maser features; bottom: rotation curve. Adapted from Ho et al. (1999).

3.2. Jets from accretion disks

Powerful, highly-collimated, oppositely directed jets are observed in AGN and quasars, and in the "microquasars" – old compact stars in X-ray binaries (Mirabel and Rodriguez, 1994). Highly collimated emission line jets are seen in young stellar objects. Different ideas and models have been put forward to explain astrophysical jets (see reviews by Begelman, Blandford and Rees, 1984; Bisnovatyi-Kogan 1993; Lovelace et al. 1999). Recent observational and theoretical work favors models

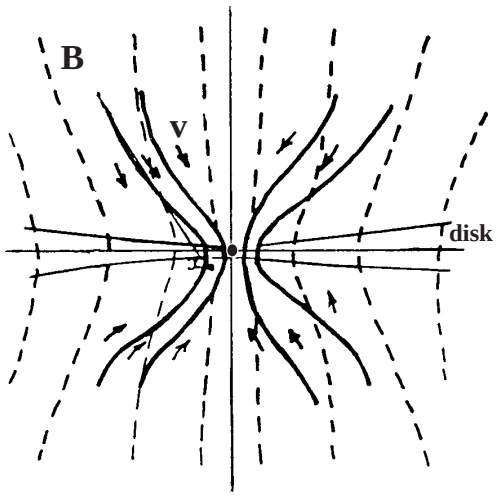

Figure 8. Sketch of the magnetic field threading an accretion disk shown increase of the field owing to flux freezing in the accreting disk matter, from Bisnovatyi-Kogan and Ruzmaikin (1976).

where twisting of an ordered magnetic field threading an accretion disk around a black hole acts to magnetically accelerate the jets as proposed by Lovelace (1976). The nature of the ordered magnetic field threading an accretion disk envisioned by Bisnovatyi-Kogan and Ruzmaikin (1976) is shown in Fig. 8. Fig. 9 shows the outflows from a disk with such an ordered field from Lovelace (1976). Jet formation in the microquasar GRS 1915+105 may be seen in Fig.10 from radio observations of Fender (1999). Picture of the jet from microquasar XTE J1550-564 obtained from X-ray satellite Chanrda are given in the paper of Kaaret et al. (2003). Formation of a jet outflowing from the accretion disk in the X-ray binary is shown schematically in Fig.11 from Fender (2001).

Observations pictures of extragalactic jets, one and two sided, are very numerous, and are obtained in several spectral bands from radio until X-rays. Two most famous jets from AGN are shown in Fig.12 (M 87, all bands), and Fig.13 (quasar 3C 273, radio). Impressive pictures in X rays obtained from Chandra are represented by Marshall et al. (2001) and Harris et al. (2003) for the jet in M 87; and by Marshall et al. (2000) and Sambruna et al. (2001) for the jet in the quasar 3C 273. The image of very extended radio jet from the nucleus of the galaxy IC 4296, with the length about 400 kpc is represented by Killen et al. (1986).

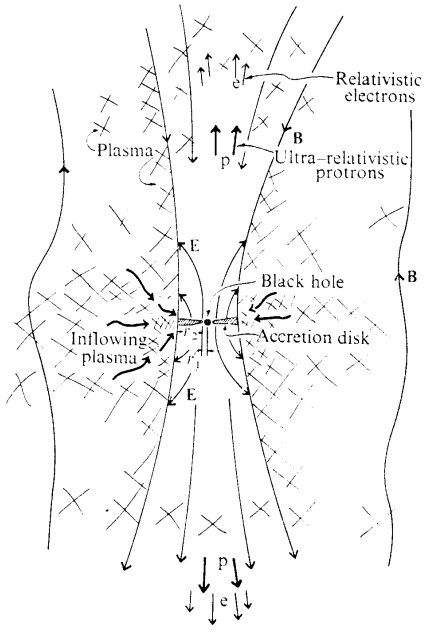

Figure 9. Sketch of the electromagnetic outflows from the two sides of the disk owing to the Faraday unipolar dynamo action of a rotating magnetized disk from Lovelace (1976).

4. Farther development of accretion theory

Few years after appearence of the standard model it was found that in addition to the opically thick disk solution there is another branch of the solution for the disk structure with the same input parameters M, $\dot{M}$, α which is also self-consistent and has a small optical thickness (Shapiro, Lightman, Eardley, 1976). Suggestion of the small optical thickness implies another equation of energy losses, determined by a volume emission

$$Q_- \approx q\,\rho\,h, \tag{14}$$

where due to the Kirchoff law the emissivity of the unit of a volume q is connected with a Plankian averaged opacity κ_p by an approximate relation $q \approx acT_0^4\kappa_p$. In the optically thin limit the pressure is determined by a gas $P = P_g$. Analytical solutions are obtained here as well, from the same equations, with volume losses and gas pressure. In the optically thin solution the thickness of the disk is larger then in the optically thick one, and density is lower.

In order to find equations of the disc structure valid in both limiting cases of optically thick and optically thin disc, and smoothly describing transition between them, Eddington approximation had been used for obtaining formulae for a heat flux and for a radiation pressure (Artemoma et al., 1996). The following expressions had been obtained for the vertical energy flux from the disc F_0, and the radiation pressure in the symmetry plane

$$F_0 = \frac{2acT_0^4}{3\tau_0}\left(1+\frac{4}{3\tau_0}+\frac{2}{3\tau_*^2}\right)^{-1}, \quad P_{rad,0} = \frac{aT_0^4}{3}\frac{1+\frac{4}{3\tau_0}}{1+\frac{4}{3\tau_0}+\frac{2}{3\tau_*^2}}, \quad (15)$$

where $\tau_0 = \kappa_e \rho h$, $\tau_* = (\tau_0 \tau_{\alpha 0})^{1/2}$, $\tau_{\alpha 0} \approx \kappa_p \rho h$. At $\tau_0 \gg \tau_* \gg 1$ we have (10) from (15). In the optically thin limit $\tau_* \ll \tau_0 \ll 1$ we get

$$F_0 = acT_0^4 \tau_{\alpha 0}, \quad P_{rad,0} = \frac{2}{3} acT_0^4 \tau_{\alpha 0}. \quad (16)$$

Using F_0 instead of Q_- and equation of state $P = \rho \mathcal{R} T + P_{rad,0}$, the equations of accretion disc structure together with equation $Q_+ = F_0$, with Q_+ from (9), have been solved numerically by Artemova et al. (1996). It occurs that two solutions, optically thick and optically thin, exist separately when luminosity is not very large. Two solutions intersect at $\dot{m} = \dot{m}_b$ and there is no global solution for accretion disc at $\dot{m} > \dot{m}_b$ (see Fig.14). It was concluded by Artemova et al (1996), that in order to obtain a global physically meaningful solution at $\dot{m} > \dot{m}_b$, account of advection is needed.

It is clear from physical ground, that when a local heat production due to viscosity goes to zero near the inner edge of the disk, the heat brought by radial motion of matter along the accretion disc becomes more important. In presence of this advective heating (or cooling term, depending on the radial entropy S gradient) written as

$$Q_{adv} = \frac{\dot{M}}{2\pi r} T \frac{dS}{dr}, \quad (17)$$

the equation of a heat balance is modified to $Q_+ + Q_{adv} = Q_-$. In order to describe self-consistently the structure of the accertion disc we should also modify the radial disc equilibrium, including pressure and inertia terms. Appearance of inertia term leads to transonic radial flow with a singular point. Conditions of a continuous passing of the solution through a critical point choose a unique value of the integration constant j_{in}. In the standard local theory $j_{in} = j_{in}^{(0)}$ corresponds to the keplerian angular momentum on the last stable orbit at $r = 3r_g$, $r_g = \frac{2GM}{c^2}$. To model the effects of general relativity the gravitational

potential of Paczynski & Wiita (1980) $\Phi = \frac{GM}{r-r_g}$ had been used in calculations of Artemova et al. (2001). For this potential

$$j_{in}^{(0)} \equiv l_{in}^{(0)} = \frac{3}{2}\sqrt{\frac{3}{2}} r_g c, \tag{18}$$

First approximate solution for the advective disc structure have been obtained by Paczynski and Bisnovatyi-Kogan (1981). Accretion disk models with advection in the optically thick limit have been constructed numerically by Abramovicz et al. (1988), and improved by Artemova et al. (2001). Add dynamical and radial pressure gradient term to the equation of radial equilibrium. Instead of Keplerian angular velocity we obtain radial hydrodynamic equation. Radial accretion flux becomes supersonic in the vicinity of the inner last stable orbit. The position of the critical radius is a proper value of the problem, differs noticeable from the radius of the last stable orbit at luminosity approaching the critical Eddington one $L_{Edd} = \frac{4\pi cGM}{\kappa}$ Relaxation method corrected for the existence of critical points had been used in calculations of Artemova et al. (2001), permitting to find solutions at large luminosity, formally exceeding the critical Eddington one. The results of these calculations are represented in Figs. 15-18.

4.1. Influence of the small-scale magnetic field on the accretion

While heating by viscosity is determined mainly by ions, and cooling is determined by electrons, the rate of the energy exchange between them is important for a thermal structure of the disk. The energy balance equations are written separately for ions and electrons. For small accretion rates and lower matter density the rate of energy exchange due to binary collisions is so slow, that in the thermal balance the ions are much hotter then the electrons. That also implies a high disk thickness.

It was noticed by Narayan and Yu (1995), that advection in this case is becoming extremely important. It may carry the main energy flux into a black hole, leaving rather low efficiency of the accretion up to $10^{-4} - 10^{-5}$ (advective dominated accretion flows - ADAF). This conclusion is valid only when the effects, connected with magnetic field annihilation and heating of matter due to it are neglected. To support the condition of equipartition during accretion a continuous magnetic field reconnection is necessary, leading to annihilation of the magnetic flux and heating of matter due to Ohmic heating. The heating of electrons during reconnection is equal or larger than ion heating. While all electron energy is emitted by magneto- bremstrahlung radiation, the efficiency of accretion cannot become less than 0.25 of its standard value

(0.06 for Schwarzschild metrics) (see Bisnovatyi-Kogan and Lovelace, 2001). In addition, in the highly turbulent plasma the energy exchange between ions and electrons may be strongly enhanced due to presence of fluctuating electrical fields, where electrons and ions gain the same energy. In such conditions difference of temperatures between ions and electrons may be negligible.

While heating by viscosity is determined mainly by ions, and cooling is determined by electrons, the rate of the energy exchange between them is important for a thermal structure of the disk. The energy balance equations are written separately for ions and electrons. For small accretion rates and lower matter density the rate of energy exchange due to binary collisions is so slow, that in the thermal balance the ions are much hotter then the electrons. That also implies a high disk thickness.

It was noticed by Narayan and Yu (1995), that advection in this case is becoming extremely important. It may carry the main energy flux into a black hole, leaving rather low efficiency of the accretion up to $10^{-4} - 10^{-5}$ (advective dominated accretion flows - ADAF). This conclusion is valid only when the effects, connected with magnetic field annihilation and heating of matter due to it are neglected. To support the condition of equipartition during accretion a continuous magnetic field reconnection is necessary, leading to annihilation of the magnetic flux and heating of matter due to Ohmic heating Bisnovatyi-Kogan and Ruzmaikin (1974). The heating of electrons during reconnection is equal or larger than ion heating. While all electron energy is emitted by magneto- bremstrahlung radiation, the efficiency of accretion cannot become less than 0.25 of its standard value (0.06 for Schwarzschild metrics) (see Bisnovatyi-Kogan and Lovelace, 2001). In addition, in the highly turbulent plasma the energy exchange between ions and electrons may be strongly enhanced due to presence of fluctuating electrical fields, where electrons and ions gain the same energy. In such conditions difference of temperatures between ions and electrons may be negligible.

5. Summary

1. Accretion into black holes (neutron stars) is a main source of energy in galactic X-ray sources and AGNs.

2. Jets, observed in AGNs and microquasars my be explained by interaction of the large-scale magnetic field with the accretion disk in self-consistent picture.

3. Accretion model deviate substantially from the standard (local) model at high accretion rates (luminosities), where advection effects are important.

4. Magnetic field action prevent formation of low-efficient flow (ADAF)

5. Turbulence in accretion disks, and turbulent viscosity is created mainly due to development of non-linear hydrodynamic instabilities at large Reynolds number.

Acknowledgements

Author is grateful to the conference organizers for support and hospitality.

References

Abramovicz, M. A., B. Czerny, J. P. Lasota, and E. Szuszkiewicz. Slim Accretion Disks *Astrophys. J.*, 332:646–658,1988.

Artemova, I. V., G. S. Bisnovatyi-Kogan, G. Björnsson and I. D. Novikov. Structure of Accretion Disks with Optically Thick–Optically Thin Transitions. *Astrophys. J.*, 456:119–123, 1996.

Artemova, I. V., G. S. Bisnovatyi-Kogan, I. V. Igumenshchev and I. D. Novikov. On the Structure of Advective Accretion Disks at High Luminosity. *Astrophys. J.*, 549:1050–1061, 2001.

Balbus S. A. and J. F. Hawley. Instability, Turbulence, and Enhanced Transport in Accretion Disks. *Rev. Mod. Phys.*, 70:1–53, 1998.

Begelman M.C., Blandford R. D. and M. J. Rees. Theory of Extragalactic Radio Sources. *Rev. Mod. Phys.*, 56:255–351, 1984.

Bisnovatyi-Kogan, G. S. X ray Sources in Close Binary Systems: Theoretical Aspects. *Bulletin Abastumani Astrophys. Obs.*, No. 58:175–210, 1985.

Bisnovatyi-Kogan, G.'S. Mechanisms of Jet Formation. In L. Errico and A. A. Vittone, editors, *Proceedings of Int. Conf. Stellar Jets and Bipolar Outflows*, 369–381, 1993. Kluwer, Dordrecht.

Bisnovatyi-Kogan G. S. and S. I. Blinnikov. Disk Accretion onto a Black Hole at Subcritical Luminosity. *Astron. Ap.*, 59:111–125, 1977.

Bisnovatyi-Kogan G. S. and R. V. L. Lovelace. Advective Accretion Disks and Related Problems Including Magnetic Fields. *New Astronomy Reviews*, 45:663–742, 2001.

Bisnovatyi-Kogan, G. S. and A. A. Ruzmaikin. The Accretion of Matter by a Collapsing Star in the Presence of a Magnetic Field. *Astrophys. and Space Sci.*, 28:45–59, 1974.

Bisnovatyi-Kogan, G. S. and A. A. Ruzmaikin. The Accretion of Matter by a Collapsing Star in the Presence of a Magnetic Field. II - Selfconsistent Stationary Picture. *Astrophys. and Space Sci.*, 42:401–424, 1976.

Cannizzo, J., P. Ghosh and J. C. Wheeler Convective Accretion Disks and the Onset of Dwarf Nova Outbursts. *Astrophys. J. Lett.*, 260:L83–L86, 1982.

Chandrasekhar, S. *Hydrodynamic and Hydromagnetic Stability*. International Series of Monographs on Physics, Oxford: Clarendon, 1961.

Chen, W., C. R. Shrader, and M. Livio. The Properties of X-Ray and Optical Light Curves of X-Ray Novae. *Astrophys. J.*, 491:312–338, 1997.

Cherepashchuk, A. M. X-ray Nova Binary Systems. *Space Sci. Rev.*, 93:473–580, 2000.

Conway, R. G., S. T. Garrington, R. A. Perley, and J. A. Biretta. Synchrotron Radiation from the Jet of 3C 273. II - The Radio Structure and Polarization. *Astron. Ap.*, 267:347–362, 1993.

Fender, R. Relativistic Jets from X-ray Binaries. *Astro-ph/9907050*, 1999.

Fender, R. Relativistic Outflows from X-ray Binaries. *Astro-ph/0109502*, 2001.

Glatzel W., Instabilities in Astrophysical Shear Flows. *Rev. in Modern Astron.*, 4:104–116, 1991.

Harris, D. E., J. A. Biretta, W. Junor, E. S. Perlman, W. B. Sparks and A. S. Wilson. Flaring X-ray Emission from HST-1, a Knot in the M87 Jet. *Astrophys. J.*, 586:L41-L44, 2003.

Ho, L. Supermassive Black Holes in Galactic Nuclei: Observational Evidence and Astrophysical Consequences. *Observational Evidence for the Black Holes in the Universe, Proc. Conference held in Calcutta, January 11-17th, 1998.*, 157–186, Kluwer, 1999.

Kaaret, P., S. Corbel, J. A. Tomsick, R. P. Fender, J. M. Miller, J .A. Orosz, A. K. Tzioumis and R. Wijnands. X-Ray Emission from the Jets of XTE J1550-564. *Astrophys. J.*, 582:945–953, 2003.

Killeen, N. E. B., G. V. Bicknell and R. D.Ekers. The radio galaxy IC 4296 (PKS 1333 - 33). I - Multifrequency Very Large Array observations. *Astrophys. J.*, 302;306–336, 1986.

Kuznetsov, O. A., G. S.Bisnovatyi-Kogan and D. Molteni. On the development of hydrodynamical turbulence in accretion discs: numerical simulations. *Month. Not. R.A.S.*, submitted, 2004.

Lasota, J.-P. The disc instability model of dwarf novae and low-mass X-ray binary transients. *New Astronomy Reviews*, 45:449–508, 2001.

Lovelace, R. V. E. Dynamo model of double radio sources. *Nature*, 262:649–652, 1976.

Lovelace, R. V. E., G. S. Ustyugova and A. V. Koldoba. Magnetohydrodynamic Origin of Jets from Accretion Disks. *Active Galactic Nuclei and Related Phenomena, IAU Symposium 194, eds. Y. Terzian, D. Weedman and E. Khachikian (Astron. Soc. of Pacific: San Francisco)*, 208–217, 1999.

Macchetto, F., A. Marconi, D. J. Axon, A. Capetti, W. Sparks and P. Crane. The Supermassive Black Hole of M87 and the Kinematics of Its Associated Gaseous Disk. *Astrophys. J.*, 489:579–600, 1997.

Marshall, H. L., D. E. Harris, J. P. Grimes, J. J. Drake A. Fruscione, M. Juda, R. P. Kraft, S. Mathur, S. S. Murray, P. M. Ogle, D. O. Pease, D. A. Schwartz, A. L. Siemiginowska, S. D. Vrtilek and B. J. Wargelin. Structure of the X-Ray Emission from the Jet of 3C 273. *Astrophys. J.*, 549:L167–L171, 2001.

Marshall, H. L., B. P. Miller, D. S. Davis, E. S. Perlman, M. Wise, C. R. Canizares and D. E. Harris. A High-Resolution X-Ray Image of the Jet in M87. *Astrophys. J.*, 564:683–687, 2002.

Mirabel, I. F. and L. F. Rodriguez. A Superluminal Source in the Galaxy. *Nature*, 371:46–48, 1994.

Miyoshi, M., J. Moran, J. Herrnstein, L. Greenhill, N. Nakai, P. Diamond, and M. Inoue. Evidence for a Black Hole from High Rotation Velocities in a Sub-parsec Region of NGC4258. *Nature*, 373:127–129, 1995.

Nandra, K., I. M. George, R. F. Mushotzky, T. J. Turner, T. Yaqoob. ASCA Observations of Seyfert 1 Galaxies. II. Relativistic Iron K alpha Emission. *Astrophys. J.*, 477:602–622, 1997.

Narayan, R. and I. Yi. Advection-dominated Accretion: Underfed Black Holes and Neutron Stars. *Astrophys. J.*, 452:710–735, 1995.

Novikov, I. D. and K. S. Thorne. Astrophysics of Black Holes. *Black Holes eds. C.DeWitt & B.DeWitt (New York: Gordon & Breach)*, 345–405, 1973.

Paczyński, B. and G. S. Bisnovatyi-Kogan. A Model of a Thin Accretion Disk around a Black Hole. *Acta Astron.*, 31:283–291, 1981.

Richard, D., F. Hersant, O. Dauchot, F. Daviaud, B. Dubrulle and J-P. Zahn. A powerful local shear instability in stratified disks. *Astro-ph/0110056*, 2001.

Sambruna, R. M., C. M. Urry, F. Tavecchio, L. Maraschi, R. Scarpa, G. Chartas and T. Muxlow. Chandra Observations of the X-Ray Jet of 3C 273. *Astrophys. J.*, 549:L161-L165, 2001.

Schwartsman, V. F. Halos around "Black Holes". *Soviet Astron.*, 15:377–388, 1971.

Shakura, N. I. Disk Model of Gas Accretion on a Relativistic Star in a Close Binary System. *Astron. Zh.*, 49:921–930, 1972 (1973, Sov. Astron. 16, 756).

Shakura, N. I. and R. A. Sunyaev. Black holes in binary systems. Observational appearance. *Astron. Ap.*, 24:337–355, 1973.

Shapiro, S. L., A. P. Lightman and D. M. Eardley. A two-temperature accretion disk model for Cygnus X-1 - Structure and spectrum. *Astrophys. J.*, 204:187–199, 1976.

Velikhov, E.P. Stability of an ideally conducting liquid flowing between rotating cylinders in a magnetic field. *J. Exper. Theor. Phys.*, 36:1398–1404, 1959.

Zeldovich, Ya. B. On the friction of fluids between rotating cylinders. *Proc. R. Soc. Lond., A* , 374:299–312, 1981.

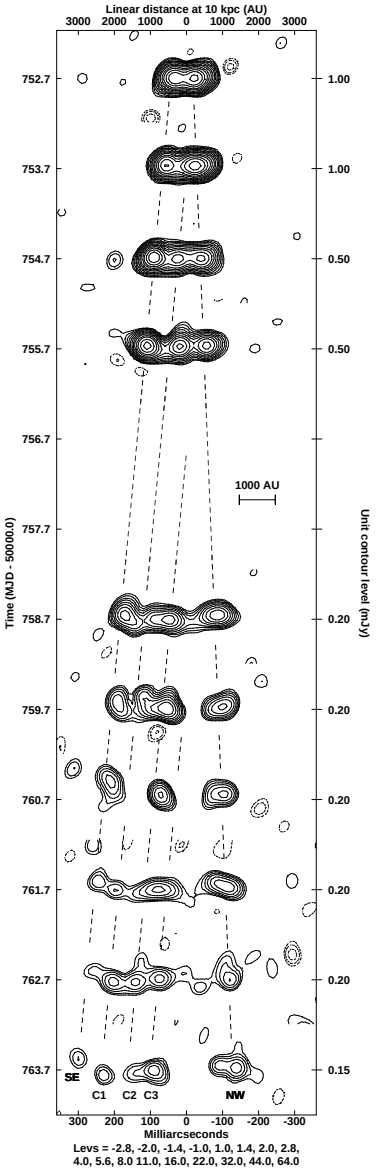

Figure 10. A sequence of ten epochs of radio imaging of relativistic ejections from the black hole candidate X-ray binary GRS 1915+105 using MERLIN at 5 GHz. The figure has been rotated by 52 degrees to form the montage. For an estimated distance to the source of 11 kpc the approaching components have an apparent transverse velocity of 1.5c. Assuming an intrinsically symmetric ejection and the standard model for apparent superluminal motions, an intrinsic bulk velocity for the ejecta is $0.98^{+0.02}_{-0.05}c$ at an angle to the line of sight of 66 ± 2 degrees (at 11 kpc). The apparent curvature of the jet is probably real, although the cause of the bending is uncertain. (from Fender, 1999).

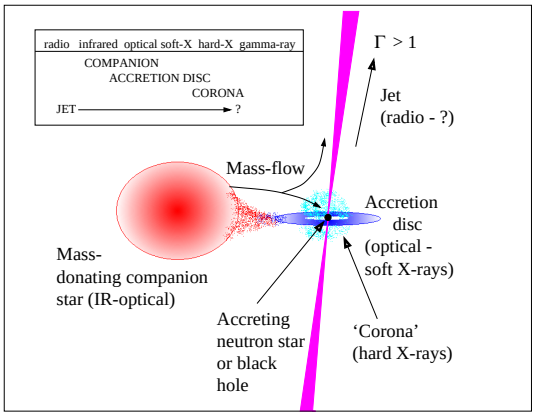

Figure 11. Schematic picture of jet formation in binary system (from Fender, 2001).

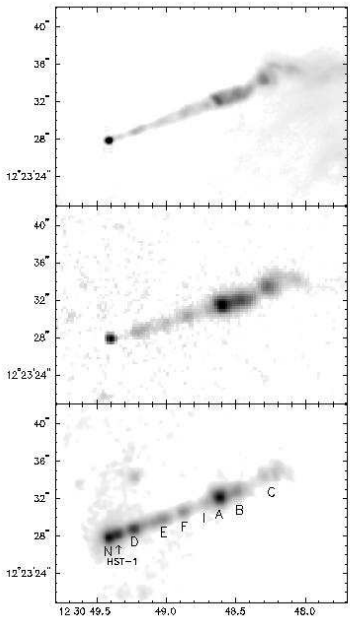

Figure 12. Grey scale representations of a 6 cm radio (top panel), an optical V band (middle panel) and the Chandra X-ray (bottom panel, 0.1 - 10 keV band) image. In the radio image, the grey scale is proportional to the square root of the brightness, in the optical image, the grey scale is also proportional to the square root of the brightness. The labels in the lower panel refer to the knots vertically above the label. N is the nucleus, from Wilson and Yang (2002).

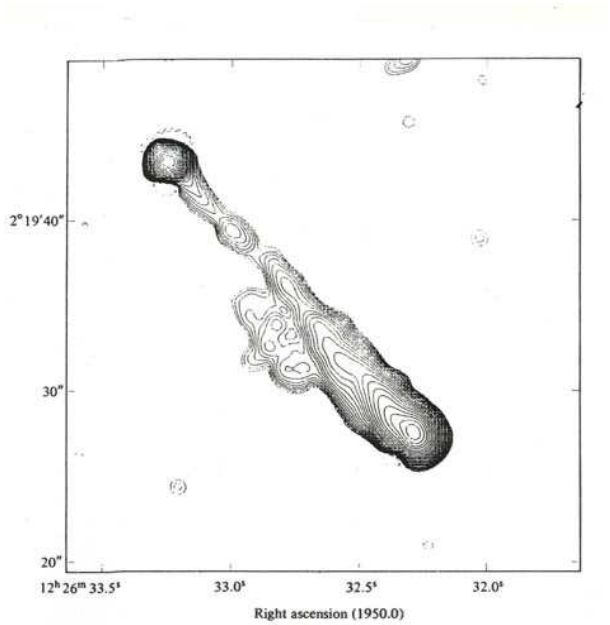

Figure 13. MERLIN map of 3C 273 at 408 MHz. Resolution: 1.0 arcsec, from Conway et al. (1993)

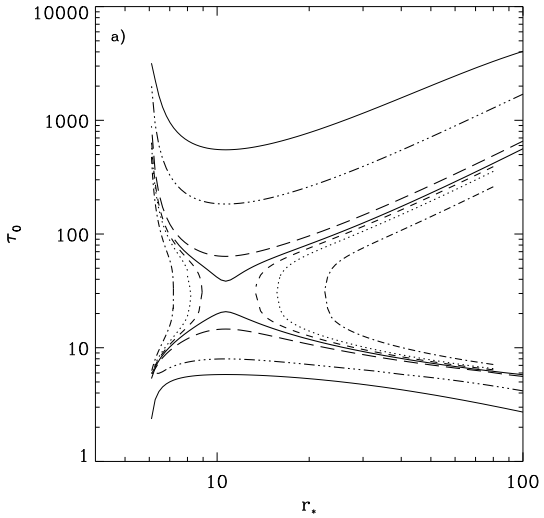

Figure 14. The dependences of the optical depth τ_0 on radius, $r_* = r/r_g$, for the case $M_{BH} = 10^8\ M_\odot$, $\alpha = 1.0$ and different values of $\dot{m}$. The thin solid, dot-triple dash, long dashed, heavy solid, short dashed, dotted and dot-dashed curves correspond to $\dot{m} = 1.0, 3.0, 8.0, 9.35, 10.0, 11.0, 15.0$, respectively. The upper curves correspond to the optically thick family, lower curves correspond to the optically thin family, from Artemova et al. (1996).

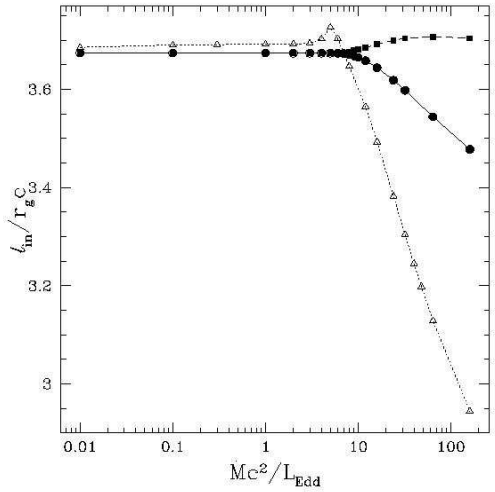

Figure 15. The specific angular momentum $j_{\rm in} \equiv \ell_{\rm in}$ as a function of the mass accretion rate $\dot{M}$ for different viscosity parameters $\alpha = 0.01$ (squares), 0.1 (circles) and 0.5 (triangles), corresponding to viscosity prescription (5). The solid dots represent models with the saddle-type inner singular points, whereas the empty dots correspond to the nodal-type ones, from Artemova et al. (2001).

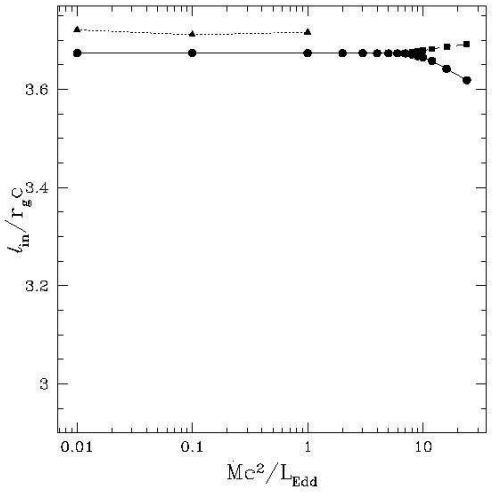

Figure 16. The specific angular momentum $j_{\rm in} \equiv \ell_{\rm in}$ as a function of the mass accretion rate $\dot{M}$ for different viscosity parameters $\alpha = 0.01$ (squares), 0.1 (circles) and 0.5 (triangles), corresponding to viscosity prescription (6). The solid dots represent models with the saddle-type inner singular points, whereas the empty dots correspond to the nodal-type ones, from Artemova et al. (2001).

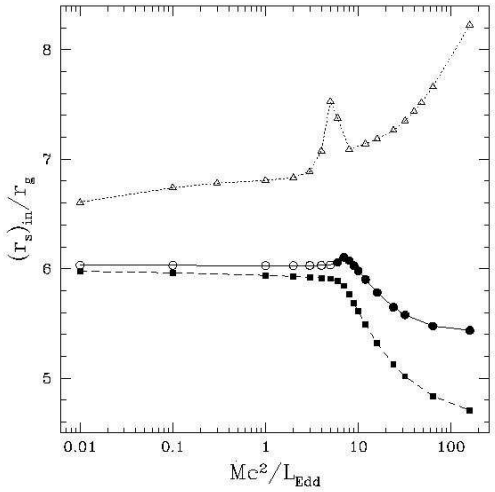

Figure 17. The position of the inner singular points as a function of the mass accretion rate $\dot{M}$ for different viscosity parameters $\alpha = 0.01$ (squares), 0.1 (circles) and 0.5 (triangles), corresponding to viscosity prescription (5). The solid dots represent models with the saddle-type inner singular points, whereas the empty dots correspond to the nodal-type ones, from Artemova et al. (2001).

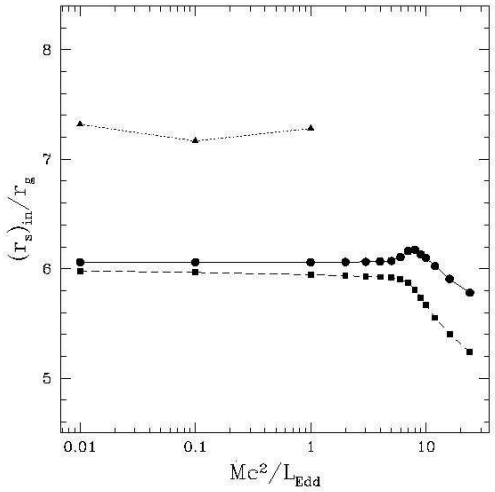

Figure 18. The position of the inner singular points as a function of the mass accretion rate $\dot{M}$ for different viscosity parameters $\alpha = 0.01$ (squares), 0.1 (circles) and 0.5 (triangles), corresponding to viscosity prescription (6). The solid dots represent models with the saddle-type inner singular points, whereas the empty dots correspond to the nodal-type ones, from Artemova et al. (2001).